Comparing Particle Filter and Extended Kalman Filter for Battery State-Of-Charge Estimation

Rocco Restaino and Walter Zamboni
Dipartimento di Ingegneria Elettronica e Ingegneria Informatica (DIEII)
Università degli Studi di Salerno
I-84084 Fisciano (SA), Italy
Email: {restaino,wzamboni}@unisa.it

***Abstract*—The battery State-Of-Charge (SOC) and parameters estimation is one of the crucial points to be addressed in the development of innovative electric/hybrid electric vehicles. Extended Kalman Filter (EKF) and Particle Filters (PF) are two possible approaches to the problem. While EKF is attractive for its computational efficiency, it may not be accurate for the non-linearity and for the uncertainties involved in the battery modelling. PF is a promising alternative, even if it is computationally more demanding. In this paper, we compare the EKF and PF performance in the dual Bayesian estimation of battery state and parameters, with particular reference to lithium batteries, showing that PF is attractive, especially in the presence of inaccurate battery models.**

I. Introduction

The Earth is suffering from air pollution and temperature increase partially due to greenhouse gas emissions, whose reduction is one of the key points of the Kyoto protocol. To address this challenge, many countries have invested a lot for the development of innovative Electric Vehicles (EV) and Hybrid Electric Vehicles (HEV). The association of an electric engine to the traditional internal combustion engines, and the use of energy accumulated in secondary batteries or provided by alternative source of energy in fuel cells and photovoltaic panels, allow to achieve the goal. The cost of the power system can reach up to one third of the total cost of the electric vehicle, and a large amount of this is due to the battery, whose cycle-life should span over the entire vehicle lifetime. In order to guarantee the battery by undesired over-/under-charge and by undesired operating conditions compromising the battery life and safety, a Battery Management System (BMS) is integrated into the power system. The BMS usually manages and protects the battery at the cell level, by measuring voltage, current and temperature of each cell. Tracking the battery state is one of the most challenging tasks required by a BMS.

The main battery state variable is the so-called battery State-Of-Charge (SOC). The SOC can be defined as the ratio of the remaining capacity to the nominal capacity of the cell, where the remaining capacity is the number of ampere-hours that can be drawn from the cell at room temperature at a sufficiently low ampere-hour rate before it is fully discharged. Obviously, from a practical point of view, SOC cannot be directly measured according to its definition without varying it dramatically. It is worth to notice that several non-matching definitions of SOC are present in the literature.

Ultimately, manufacturers of HEVs would like predictions of the State-Of-Health (SOH) or State-Of-Function (SOF) of a battery pack [1], since the increasing reliance on drive-by-wire technologies is making the battery a key safety-critical component of the vehicle. SOH monitoring techniques are currently in their infancy (see [2] and reference therein).

A wide variety of monitoring techniques have been proposed to measure the SOC of a cell or battery [3]. Coulomb counting (charge counting) or current integration is, at present, the most commonly used technique, requiring dynamic measurement of the cell/battery current, the time integral of which is considered to provide a direct indication of SOC [4]. This is basically an open-loop technique, and, due to the reliance on integration, errors in terminal measurements due to noise, resolution, and rounding are cumulative and large SOC errors can result, calling either for a recalibration action or for a compensation at regular intervals. This is less appropriate for standard EV-HEV operation, where full SOC is rarely achieved. The variation of cell capacity with discharge rate, temperature, and Coulombic efficiency losses are additional factors that ultimately influence the accuracy of SOC estimates with the integration method.

Specific gravity of the electrolyte is known to be a good measure of SOC for lead-acid batteries (except for Valve Regulated Lead Acid (VRLA) batteries) to be performed during periods of vehicle operational inactivity. VRLA batteries may benefit from the use of the Open Circuit Voltage (OCV) as a SOC indicator, being the SOC-OCV curve almost linear in the central region. However, as with measurements of specific gravity, suitable periods of operational inactivity may not occur frequently enough in vehicle driving duties for this to be successfully utilized, and corrections for high charge-discharge rate are needed. Cell-impedance measurements might help in resetting or adjusting SOC estimates from integration-based methods. However, from results of various studies undertaken to identify the impedance variation of cells/batteries with SOC [5], [6], [7], contradictory views to their usefulness in practical systems currently remain unresolved [3].

An alternative approach is based on a black box battery models that describe the nonlinear relationship between the SOC and its influencing factors, which can often produce

978-1-4673-2421-2/12/$31.00 ©2012 IEEE

a good estimate of the SOC due to the powerful ability to approximate nonlinear function surfaces, with the drawback of heavy computational burden and bad real-time application (e.g., methods based on artificial neural networks and fuzzy logic principles [8]-[9]). These approaches typically require large computation overhead on the digital signal processors controlling the battery pack, but the increasing computational capacity and the cost reduction of the commercially available parts make these methods attracting.

A very effective approach to the battery monitoring is based on state estimation techniques with state space battery models, which is popular due to the advantages of being close-loop, allowing online estimation, and available to dynamically regulate the estimation error range. The Kalman Filter (KF) algorithm and its derived methods [10]-[11] can be used to implement online SOC estimation on the basis of the chosen model, as well as the parameter identification of the model itself. It is worth to highlight that this might include the estimation of SOH through the tracking of the drift of some key model parameters [12]-[13]. In particular, KF is suitable for dynamic driving conditions. A correct setting of the predetermined variables of the system noise may help in favoring the desired convergence of the method. Notice that all filters based on KF approach strongly depend on the accuracy of the battery state-space model. From one hand, one might desire a very sophisticated model for a specific battery, to guarantee high accuracy of the filter estimation in this peculiar case. But, on the other hand, this reduces the versatility of the estimator (and of the related device implementing the estimate), which may result useless for another type of battery.

For nonlinear systems, as battery models are, or in the presence of non-Gaussian noise, there is no general analytic (closed form) solution for the state space probability density function (pdf), but the modified form of the KF, namely the Extended Kalman Filter (EKF), keeps being among the most popular solutions. In KF/EKF, the desired pdf is assumed to be Gaussian and, accordingly, the first and second order moments completely specify its functional form. This may results in significant deviation from the true distribution causing the filter to diverge. A credited alternative for dealing with non linear/non Gaussian models is the Particle Filter (PF). In the latter, the pdf is approximated by a set of particles (points) representing the support of the state distribution, and a set of associated weights denoting discrete probability masses [14]. The particles are generated and recursively updated from a nonlinear process model that describes the evolution in time of the system under analysis, a measurement model, a set of available measurements and an *a priori* estimate of the state pdf. In other words, PF is a technique for implementing a recursive Bayesian filter by using Monte Carlo simulations.

In this work, we compare the performance of PF – promising for the non linearity involved in the battery models – and EKF – well assessed for such an application. We show the peculiar advantages of a PF in the framework of battery state and parameter dual estimation, with particular reference to lithium battery (cell) models.

II. Battery Modelling

We assume that the battery SOC is defined by the basic Coulomb counting time integral:

$$z(t) = z(0) - \int_0^t \frac{\eta i(\tau)}{C}\, d\tau \tag{1}$$

where $z \in [0,1]$ is the battery SOC, t is the time, i is the current flowing through the battery ($i > 0$ for discharge process), C is the nominal battery capacity, η is the charge/discharge efficiency ($\eta = 1$ for discharge, $\eta < 1$ for current charging the battery). The corresponding discrete time equation, achieved with a sampling interval Δt, is:

$$z_{k+1} = z_k - \frac{\eta \Delta t}{C} i_k. \tag{2}$$

A. Pseudo-Thévenin Model

The terminal voltage v is given by:

$$v_k = \mathrm{OCV}(z_k) - R i_k, \tag{3}$$

where the Open Circuit Voltage (OCV) is related to the battery SOC through a given function, such as the one plotted in Figure 1(a), and the series resistance R may depend on the current sign (we indicate it with the symbol R^+ if $i > 0$, and with R^- if $i < 0$).

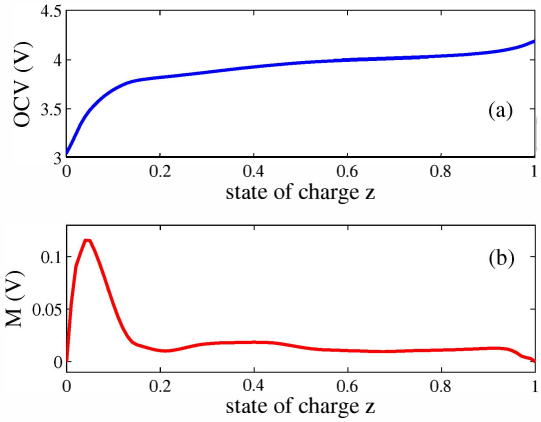

Fig. 1. (a) Battery OCV as a function of the SOC (the curve is obtained by a complete low current charge-discharge cycle set of data). (b) Battery maximum hysteresis as a function of the SOC.

B. Dynamic Hysteresis Model

In lithium battery, the charge curve $\mathrm{OCV_c}(z)$ lies above the discharge curve $\mathrm{OCV_d}(z)$ in the z-OCV plane: this is often called battery hysteresis, and it is a dynamic phenomenon [15]. The half of the difference M between branches is called maximum hysteresis, and it is again a function of z (intrinsically positive by definition):

$$M(z) = \frac{1}{2}\left[\mathrm{OCV_c}(z) - \mathrm{OCV_d}(z)\right], \tag{4}$$

while the average curve $\mathrm{OCV}(z)$ is:

$$\mathrm{OCV}(z) = \frac{1}{2}\left[\mathrm{OCV_c}(z) + \mathrm{OCV_d}(z)\right]. \tag{5}$$

The hysteresis m is positive for charge and negative for discharge:

$$m(z, \dot{z}) = -\mathrm{sgn}(i)M(z) = \mathrm{sgn}(\dot{z})M(z); \tag{6}$$

moreover, it is subject to a time delay with respect to the forcing current. The phenomenon is well modelled by the following equation:

$$\frac{dh(z,t)}{dz} = \gamma\,\mathrm{sgn}(\dot{z})\left[M(z) - h(z,t)\right], \tag{7}$$

where h is the hysteresis voltage affecting the output voltage v (it acts as a controlled voltage source), and γ is a characteristic constant. The state space equation (7) leads to the following time domain equation:

$$\frac{dh(z,t)}{dt} = -\Gamma h(t) + \mathrm{sgn}(\dot{z})\Gamma M(z) \tag{8}$$

where we have defined:

$$\Gamma = \frac{\eta|i|\gamma}{C} \tag{9}$$

In discrete time we obtain:

$$h_{k+1} = \Gamma h_k + \mathrm{sgn}(i)(1-\Gamma)M(z) \tag{10}$$

together with the output equation:

$$v_k = \mathrm{OCV}(z_k) - Ri_k + h_k. \tag{11}$$

The model described above is called Dynamic Hysteresis Model (DHM). The model can be further improved by adding relaxation dynamics. However, to avoid managing and reporting about more state variables and parameters, for the sake of simplicity, we assume the DHM as the reference model.

III. Dual Bayesian Estimation

In dual estimation, two parallel interacting dynamic systems are assumed to be in force; the first one models the trajectory of the state, consisting of the SOC z and, eventually, of the hysteresis h. The state x and the output y evolve according to the state and measurement equations:

$$x_{k+1} = \mathcal{F}(x_k, u_k, q_k) + \xi_k, \tag{12}$$

$$y_k = \mathcal{G}(x_k, u_k, q_k) + \phi_k, \tag{13}$$

being u_k and q_k the model input and parameters at time k, and ξ_k and ϕ_k the state and measurement noises, with zero mean and covariance matrix Σ_k^{ξ} and Σ_k^{ϕ}, respectively. Given a sequence of observations $\{y_k\}_{k=0,\ldots,N} \equiv y_{0:N}$, the optimal Bayesian estimator is achieved by maximizing the posterior density $p(x_{0:N}|y_{0:N})$ of the whole state trajectory $\{x_k\}_{k=0,\ldots,N} \equiv x_{0:N}$:

$$\hat{x}_{0:N} = \arg\max_{x_{0:N}}\{p(x_{0:N})\}. \tag{14}$$

However, under mild Markovianity hypotheses, $p(x_{0:N}|y_{0:N})$ can be recursively calculated into two successive steps: the state distribution at time k, given the observation until time $k-1$, can be obtained by maximizing the posterior density

$$p(x_k|y_{0:k-1}) = \int p(x_k|x_{k-1})\, p(x_{k-1}|y_{0:k-1})\, dx_{k-1}, \tag{15}$$

in which $p(x_k|x_{k-1})$ is the state transition probability. Finally, the state distribution at time k, given the observation until time k, is given by the Bayes theorem:

$$p(x_k|y_{0:k}) = \frac{p(y_k|x_k)p(x_k|y_{0:k-1})}{p(y_k|y_{0:k-1})}, \tag{16}$$

where $p(y_k|x_k)$ is the likelihood function and $p(y_k|y_{0:k})$ is a normalizing constant.

Analogously, the evolution of parameters and the corresponding observations are described by a second couple of equations:

$$q_{k+1} = q_k + \chi_k, \tag{17}$$

$$y_k^* = \mathcal{G}(x_k, u_k, q_k) + \psi_k. \tag{18}$$

where χ_k and ψ_k are the state and measurement noise, with zero mean and covariance matrix Σ_k^{χ} and Σ_k^{ψ}, respectively. Notice that, although the measurement equation (18) uses the function $\mathcal{G}$ also appearing in (13), the time step at which it is computed *may* differ from that used in (13). So, the output variable is affected, in principle, by another measurement noise. Note also that, since the parameters are deterministic quantities, a common practice for recasting the problem in the Bayesian framework entails an identity transition operator for the parameters and the introduction of a fictitious noise χ_k.

The dual estimation approach [16] consists in following the two dynamic evolutions concurrently, namely in using two separate sequential filters to estimate the state and parameters values through time. The dual estimation is often performed by running two KFs that yield the estimate and the error covariance matrix of state and parameters. Only for linear Gaussian statistical models, this method turns out to provide the optimal Bayesian solution. However it is very effective also in the presence of non linear equations and/or non-Gaussian distributions, as confirmed by the results achieved for battery state and parameters estimation [17]. Specifically, this application requires the use of the more general EKF, that corresponds to apply the KF to the state and measurement equation linearized about the current estimates.

Let $\hat{x}_{k|j}$ and $\hat{q}_{k|j}$ indicate the state and parameters estimate at time k, given observations until time j, respectively, and $\Sigma_{k|j}^x$, $\Sigma_{k|j}^q$ the corresponding error covariances; the dual EKF estimation algorithm relies upon the following recursion [18]. Initialize with:

$$\begin{aligned} \hat{q}_{0|0} &= E[q], \quad \Sigma_{0|0} = E[(q-\hat{q}_{0|0})(q-\hat{q}_{0|0})^T], \\ \hat{x}_{0|0} &= E[x], \quad \Sigma_{0|0} = E[(x-\hat{x}_{0|0})(x-\hat{x}_{0|0})^T]. \end{aligned}$$

For $k \geq 1$ propagate the parameter and state estimates according to:

$$\hat{q}_{k|k-1} = \hat{q}_{k-1|k-1}, \tag{19}$$

$$\Sigma_{k|k-1}^q = \Sigma_{k-1|k-1}^q + \Sigma_k^{\chi} \tag{20}$$

and

$$\hat{x}_{k|k-1} = \mathcal{F}(\hat{x}_{k-1|k-1}, u_k, \hat{q}_{k|k-1}), \tag{21}$$

$$\Sigma^x_{k|k-1} = F_{k-1}\Sigma^x_{k-1|k-1}F^T_{k-1} + \Sigma^\xi_k. \tag{22}$$

Then use measurements to update the state and the parameters through equations

$$L^x_k = \Sigma^x_{k|k-1}(C^x_k)^T[C^x_k\Sigma^x_{k|k-1}(C^x_k)^T + \Sigma^\phi_k]^{-1}, \tag{23}$$

$$\hat{x}_{k|k} = \hat{x}_{k|k-1} + L^x_k[y_k - \mathcal{G}(\hat{x}_{k|k-1}, u_k, \hat{q}_{k|k-1})], \tag{24}$$

$$\Sigma^x_{k|k} = (I - L^x_k C^x_k)\Sigma^x_{k|k-1} \tag{25}$$

and

$$L^q_k = \Sigma^q_{k|k-1}(C^q_k)^T[C^q_k\Sigma^q_{k|k-1}(C^q_k)^T + \Sigma^\psi_k]^{-1}, \tag{26}$$

$$\hat{q}_{k|k} = \hat{q}_{k|k-1} + L^q_k[y_k - \mathcal{G}(\hat{x}_{k|k-1}, u_k, \hat{q}_{k|k-1})], \tag{27}$$

$$\Sigma^q_{k|k} = (I - L^q_k C^q_k)]\Sigma^q_{k|k-1}. \tag{28}$$

In the previous formulas L^x_k and L^q_k are the state and parameters Kalman gains, and the matrices F_k, C^x_k and C^q_k are achieved by linearizing equations (12), (13) and (18), respectively, and thus they are defined as:

$$F_k = \left.\frac{d\mathcal{F}(x, u_k, \hat{q}_{k+1|k})}{dx}\right|_{x=\hat{x}_{k|k}}, \tag{29}$$

$$C^x_k = \left.\frac{d\mathcal{G}(x, u_k, \hat{q}_{k+1|k})}{dx}\right|_{x=\hat{x}_{k|k-1}}, \tag{30}$$

$$C^q_k = \left.\frac{d\mathcal{G}(\hat{x}_{k|k-1}, u_k, q)}{dq}\right|_{q=\hat{q}_{k|k-1}}. \tag{31}$$

Being $\hat{x}_{k|k-1}$ function of the parameters, C^q_k requires the following recurrent calculation:

$$\frac{d\mathcal{G}(\hat{x}_{k|k-1}, u_k, q)}{dq} = \frac{\partial\mathcal{G}(\hat{x}_{k|k-1}, u_k, q)}{\partial\hat{x}_{k|k-1}}\frac{d\hat{x}_{k|k-1}}{dq} + \frac{\partial\mathcal{G}(\hat{x}_{k|k-1}, u_k, q)}{\partial q}, \tag{32}$$

$$\frac{d\hat{x}_{k|k-1}}{dq} = \frac{\partial\mathcal{F}(\hat{x}_{k-1|k-1}, u_k, q)}{\partial\hat{x}_{k-1|k-1}}\frac{d\hat{x}_{k-1|k-1}}{dq} + \frac{\partial\mathcal{F}(\hat{x}_{k-1|k-1}, u_k, q)}{\partial q}, \tag{33}$$

$$\frac{d\hat{x}_{k-1|k-1}}{dq} = \frac{d\hat{x}_{k-1|k-2}}{dq} - L^x_{k-1}\frac{d\mathcal{G}(\hat{x}_{k-1|k-2}, u_{k-1}, q)}{dq}, \tag{34}$$

in which it was assumed that L^x_k is not a function of p.

To deal with the nonlinearity of the state and observation models described in Section II, numerous enhancements to the basic procedure have been developed (*e.g.*, [19], [20]). The most credited solution in the presence of non linear/non-Gaussian statistical models is represented by the particle filter [21]. It is based on a discrete approximation of the state posterior pdf, that, for example in the case of the battery state, is written as

$$p(x_k|y_{0:k}) \simeq \sum_{i=1}^{n} w^i_k\delta(x_k - x^i_k) \tag{35}$$

in which $\delta(\cdot)$ is the Dirac delta measure and $\{x^i_k\}_{i=1,\ldots,n}$ is a set of n support points (or *particles*), with associated normalized *weights* $\{w^i_k\}_{i=1,\ldots,n}$. We use in this paper its most widely used form, namely the Sequential Importance Resampling (SIR) paradigm (see [22] for a wide review of alternative possible implementations), in which the i-th particle at time k is generated according to the transition probability $p(x_k|x^i_{k-1})$. This assumption implies also a very simple form for the weight update equation, that turns out to be the following

$$w^i_k \propto w^i_{k-1}p(y_k|x^i_k). \tag{36}$$

A crucial point is represented by the degeneracy problem, namely the tendency of all but a few particles to have negligible weights. This phenomenon can be mitigated by performing a resampling step in which a greater number of particles are associated with the support points with large weights. To avoid an excessive increase of computational burden, the effective sample size

$$N_{\text{eff}} = \frac{1}{\sum_{i=1}^{n}(w^i_k)^2} \tag{37}$$

is used as a quantitative measure of degeneracy and the resampling is performed only when N_{eff} is below a given threshold.

IV. Numerical Results

The dual estimation methods based on the EKF and on the PF-SIR are compared here in some numerical experiments, where a real battery (the physical system) is emulated by running the non linear system described by the DHM. We have: $x_{\text{xp}} = [z, h]^T$, $q_{\text{xp}} = [R^+, R^-, \gamma]^T$, and $y_{\text{xp}} = v$ (the subscript xp indicate emulated experimental variables). A Gaussian measurement noise having variance σ^2_v is added to the deterministic output voltage obtained by the model. The values of the parameters are: $R^+ = 5$ mΩ, $R^- = 5$ mΩ, $\gamma = 1000$, while the OCV and the maximum hysteresis are represented in Figures 1(a)(b), respectively. Such an approach takes the advantage of the exact knowledge of the battery SOC, which would be subject to a further uncertainty if computed with an alternative method, *e.g.*, compensated Coulomb counting. No noise is added to the process equation, so the battery SOC z and hysteresis h are those provided directly from (2) and (10). Notice that such a SOC is used in the following figures as a reference variable.

The input u is the current i in Figure 2. It is derived from the vehicle speed of a city test defined by the U.S. Enviromental Protection Agency (Urban Dynamometer Driving Schedule (UDDS) [23]), in the hypothesis of a hybrid vehicle with regenerative braking. The input current is repeated N_{rep} times.

It is worth to notice that both filters require a battery model. From a practical point of view, using the same model for the generation of the emulated experimental data, as well as for the state and parameter estimation, guarantees the best filter performances. But in the real practice, this condition is never fulfilled, because the physical system rarely behaves as an ideal system. So, in the following numerical tests, we allow

the model used for the filters to coincide – or not – with that used in the generation of the set of emulated experimental data. Accordingly, the model used by the filter will be specified for each numerical test.

A. Example 1. Consistency Between SIR and EKF Approaches

In the first numerical example, we check the consistency of the approaches and compare the filter recovery speed when starting from a deeply uncorrect initialization on both SOC and parameters (emulating a very initial use of the filter for a specific battery). From a practical point of view, such a big mismatch can be limited by starting from the set of "last achieved" state and parameters.

The battery model used by the filter in this example is the DHM (it coincides with that used for "true" system). So, $x = [z, h]^T$, $q = [R^+, R^-, \gamma]^T$, and $y = v$. Both the OCV and maximum hysteresis curves are those in Figure 1. Here, we set: $N_{\text{rep}} = 10$, $\sigma_v^2 = 10^{-3}\,V^2$, and the initial guess are: z_0=0.70 instead of 0.95, and $R_0^+ = 1$ mΩ, $R_0^- = 9$ mΩ, $\gamma_0 = 100$). The variances are set as follows: $\sigma_i^2 = 10^{-3}\,A^2$; $\sigma_z^2 = 10^{-6}$; $\sigma_h^2 = 10^{-8}\,V^2$; $\sigma_R^2 = 10^{-4}\,\Omega^2$; $\sigma_\gamma^2 = 10^{-4}\,\Omega^2$; the subscripts indicate the reference variable.

Figure 3 shows the battery SOC and parameter R^+ estimation. EKF shows faster initialization error recovery with respect to SIR, for almost the same regime rms error (1.1%, evaluated with Monte Carlo simulation). 500 particles are used in SIR (in several tests, simulation with 1000 particles have shown almost the same errors), which implies a +102% increase of the computational time with respect to EKF.

B. Example 2. Effects of measurement errors on OCV curve

The battery is modelled again with the DHM (γ is set to its correct value, and the related variance is drastically reduced to keep it almost constant). Then, we add to the OCV curve depicted in Figure 1(a) a small Gaussian noise having variance equal to $5 \cdot 10^{-3}\,V^2$. This represents the uncertainty due to the measurement and the acquisition process. Although the dispersion of the SOC-OCV points is not appreciable on a

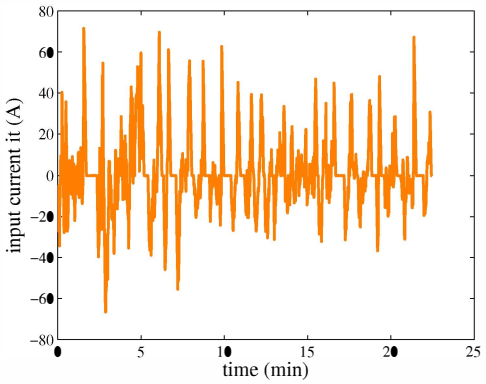

Fig. 2. Battery current in a hybrid electric vehicle derived from a typical city driving test (EPA UDDS).

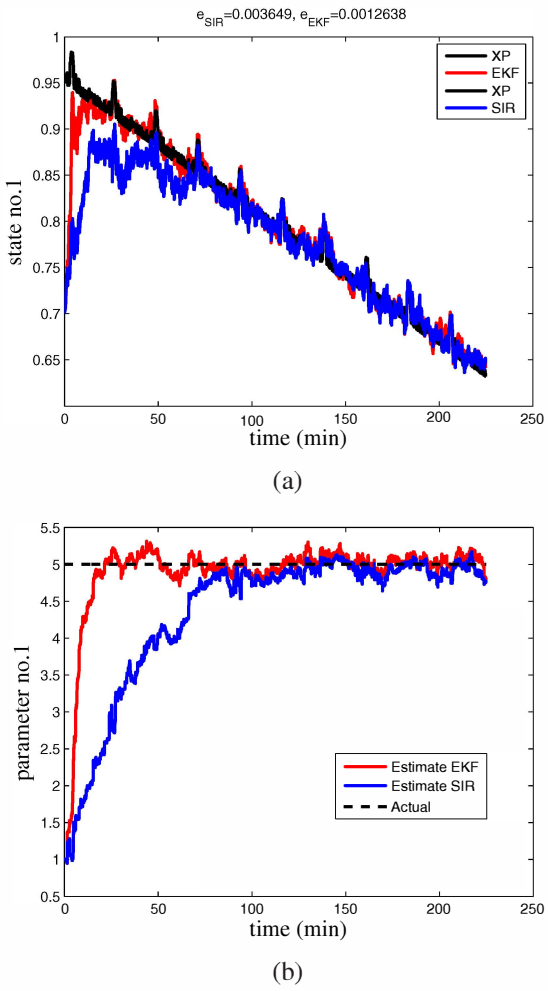

Fig. 3. Estimation of the battery state of charge (a) and parameter R_+ (b) using EKF and SIR. The DHM is used by both filters.

diagram, this noise lead to oscillating derivatives, which may affect the performance of the EKF.

Figure 4 shows the absolute error on SOC estimation. The accuracy of the EKF is outperformed by SIR, which does not use the numerical derivative of the OCV. The regime rms errors, evaluated with Monte Carlo method, is 2.4% for EKF, and 1.0% for SIR (using 500 particles). The computational costs are almost the same quoted for Example 1.

C. Example 3. Effects of a Lack in the Battery Modelling

From a practical point of view, the necessity of using a model suitable for several kinds of batteries may require the use of very simple model, such as the pseudo-Thévenin one. In this example we use the latter, based on a reduced state $x = z$ and on the same output $y = v$. The model includes only a subset of the parameters present in the DHM: $q = [R^+, R^-]^T$. The OCV curve keeps being affected by a Gaussian noise.

In this case, the dual filter is not expected to "exactly" estimate the parameters, since they have to account also for the modelling "lacks". We starting from a correct initial guess on the battery SOC ($z_0 = 0.95$). Indeed, Figure 5(b) shows

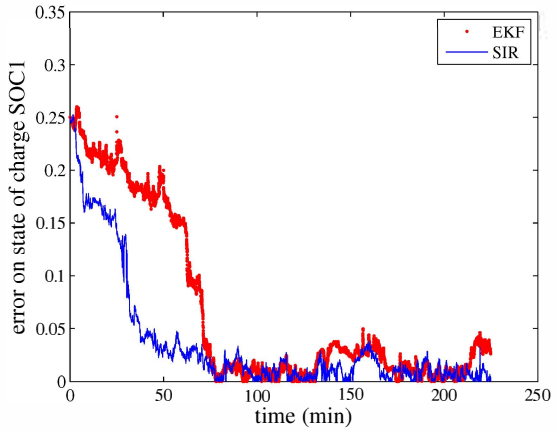

Fig. 4. Estimation error on the battery state of charge using EKF and SIR. The DHM is used by both filters, and the OCV curve is affected by a measurement error.

that R^+ tends to be overestimated. Since the hysteresis has been neglected, this result turns out to be expected. SOC and SOC estimation error are reported in Figure 5(a)(c). Again, EKF suffers from more oscillations, and its Monte Carlo rms error is higher than that of SIR (4.6% versus 1.6%), while SIR is slower. The additional computational time required for SIR is +53% (notice that the cardinality of the state is half of that in Example 1 and 2).

V. Conclusions

Three numerical examples are presented to compare the performance of the EKF and the SIR particle filter in the framework of battery state and parameter dual Bayesian estimation. Although the EKF is faster in terms of initialization error recovery in the presence of an accurate modelling of the battery, the SIR appears more robust than EKF when the model data are affected by Gaussian noise, as it often happens if they are collected by experimental data. Such a behaviour is further highlighted when a rougher model is used to represent the battery characteristics.

References

[1] Meissner, E.; Richter, G., *J. Power Sources*, Vol. 116, pp. 79-98, 2003.
[2] B. Saha, K. Goebel, S. Poll, J. Christophersen, "An integrated approach to battery health monitoring using bayesian regression and state estimation," *Proc. of IEEE Autotestcon*, pp. 646-53, 2007.
[3] S. Piller, M. Perrin, and A. Jossen, *J. Power Sources*, Vol. 96, pp. 113-120, 2001.
[4] V. Pop *et al.*, *Meas. Sci. Technol.*, Vol. 16, R93R110, 2005.
[5] H. Blanke *et al.*, *J. Power Sources*, Vol. 144, no. 2, pp. 418-425, 2005.
[6] F. Huet, *J. Power Sources*, Vol. 70, pp. 59-69, 1998..
[7] S. Rodrigues *et al.*, *J. Power Sources*, Vol. 87, pp. 12-20, 2000.
[8] M. Charkhgard, M. Farrokhi, *IEEE T. Ind. Electron.*, Vol. 57, No. 12, pp. 4178–4187, 2010.
[9] W. X. Shen *et al.*, *IEEE T. Ind. Electron.*, Vol. 49(3), pp. 677684, 2002.
[10] Kalman, R. E., *J. Basic Eng.-T ASME*, Vol. 82, No. 1, pp. 35–45, 1960.
[11] D. Simon, *Optimal State Estimation. Kalman, H_∞, and Nonlinear Approaches*, Wiley, 2005.
[12] H. He *et al.*, *IEEE T. Veh. Technol.*, Vol. 60, No. 4, pp. 1461-9, 2011.
[13] B. S. Bhangu *et al.*, *IEEE T. Veh. Technol.*, Vol. 54(3), pp. 783-94, 2005.
[14] M. Gao, Y. Liu, Z. He, "Battery state of charge online estimation based on particle filter," *Proc. of CISP 2011*, Vol. 4, pp. 2233-2236, 2011.

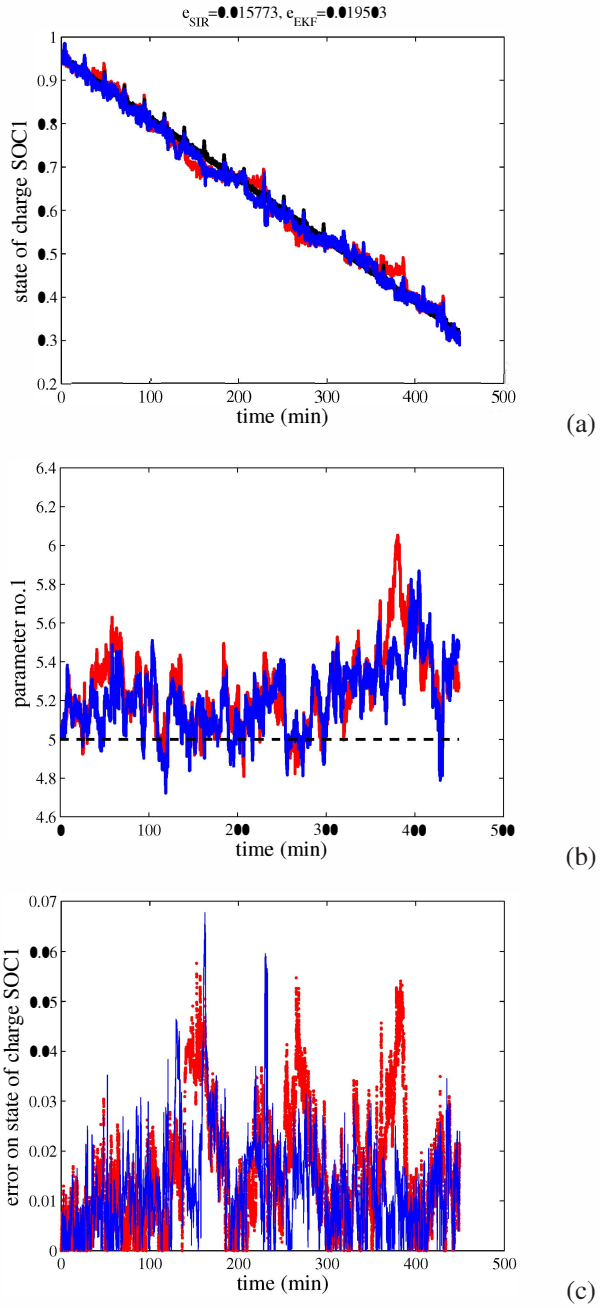

Fig. 5. SOC, R^+ and estimation error on the battery state of charge using EKF (red) and SIR (blue). The filters use a pseudo-Thévenin model, and the OCV curve is affected by a measurement error

[15] G. L. Plett, *J. Power Sources*, Vol. 134, pp. 262-276, 2004..
[16] L. W. Nelson; E. Stear, *IEEE T. Automat. Contr.*, Vol. 21, No. 1, pp. 94–98, 1967.
[17] G. L. Plett, *J. Power Sources*, Vol. 134, pp. 277-292, 2004..
[18] E.A. Wan, A.T. Nelson, "Dual Extended Kalman Filter Methods," *in S. Haykin Ed., Kalman Filtering and Neural Networks*, pp. 271–320, John Wiley & Sons, 2001.
[19] G. L. Plett, *J. Power Sources*, Vol. 161, pp. 1369-1384, 2006.
[20] S. Santhanagopalan, R. E. White, *Int. J. Energy Res.*, 34:152163, 2010.
[21] N. J. Gordon, D.J. Salmond, A.F.M. Smith, *Radar and Signal Processing, IEE Proceedings F*, Vol. 140(2), pp. 107-113, 1993.
[22] S. Arulampalam *et al.*, *IEEE T. Signal Proces.*, Vol. 50,pp. 174-88,2002.
[23] Available online at: http://www.epa.gov/nvfel/testing/dynamometer.htm